

An Empirical Analysis of IEEE 802.11ax

Siraj Muhammad, Jiamiao Zhao, and Hazem H. Refai

Electrical and Computer Engineering

University of Oklahoma

Tulsa, OK, USA

{sirajmuhammad, jiamiaoz, hazem}@ou.edu

Abstract—An empirical analysis of the newly released standard IEEE 802.11ax, widely known as Wi-Fi 6, is presented in this paper. Several tests were conducted to evaluate key performance metrics, including throughput and jitter as a function of network parameters (e.g., packet size and window size), as well as environment variables (e.g., SNR). Empirical models were developed using collected results to quantify the behavior of said metrics. Channel utilization of the system was also investigated and compared to its precedent, 802.11ac.

Index Terms—Wi-Fi, 802.11ax, WLAN, throughput, jitter, channel utilization

I. INTRODUCTION

Wireless connectivity is essential today and, in the future, as it facilitates unplugging excessive wires from conventional instruments, adds mobility to others, and transforms appliances into smart gadgets. From smart phones to smart TVs, medical devices to connected cars and autonomous vehicles, and the revolution of the internet of things (IoT), each wireless device depends on its ability to reliably and quickly communicate massive amounts of data from one point to another. For the past two decades, wireless data transport has been achieved largely by the 802.11 standard family, specifically the 802.11a/b/g/n variants. This standard has matured over the years, improving achieved throughput, enhancing channel access schemes, and accommodating an increasing number of users. While these improvements have kept current with demand, society is being ever more inundated by a massive number of connected devices.

According to statistical studies, the number of connected devices has been exponentially increasing for the past 10 years. Aruba Networks reported that 50% of all internet traffic was carried by Wi-Fi technology in 2018 [1]. The remaining traffic has been supported by LTE. According to an Ericsson report, traffic generated by smartphones in 2022 is expected to increase 10 times the amount reported in 2016 [2]. This translates into more than 60 exabytes of data per month. This extensive amount of data flow is attributed mainly to new use cases of wireless connectivity projected for the next five years (e.g., online gaming, virtual reality (VR), critical services and infrastructure control, sensor networks, and smart transportation). The automotive domain has experienced a surge in WLAN-equipped vehicles, and researchers have investigated the feasibility of Wi-Fi access points in such scenarios [3], [4]. Such applications rely

on three main characteristics of next generation wireless communications, namely ultra-low-latency, extremely high bandwidth, and massive density. In the licensed spectrum domain, 5G New Radio (NR) is the answer to new requirements. Device-to-Device (D2D) communication is regarded as a potential LTE technology to address spectrum scarcity in ultra-dense heterogeneous networks [5]. To address demands in the unlicensed spectrum, domains such as Free-Space Optical (FSO) communication are going through active research to supplement high bit rate multi-user links [6]. To this end, the IEEE standardization body introduced a new member to its 802.11 family, namely “802.11ax High-Efficiency,” or Wi-Fi 6.

Khorov, et. al [7] described key features of the latest Wi-Fi breakthroughs with particular focus on the draft D3.0 of the 802.11ax standard, which was released in May 2018. Orthogonal Frequency Division Multiple Access (OFDMA) is the cornerstone advancement of the standard and is aimed to address the throughput bottleneck at the Medium Access Control (MAC) layer.

Qu [8] analyzed the way in which OFDMA coordinated access point and devices, ensuring a node can simultaneously transmit or receive. The researchers developed a MAC protocol, including new physical layer sensing, fast back-off process, enhanced RTS/CTS mechanism, and frame structures, as well as a mathematical model to predict maximum throughput by leveraging the new MAC protocol. Results proved that maximum throughput increased by 160%.

Naik [9] studied the uplink multi-user (MU) OFDMA and derived an analytical model using Bianchi’s Markov Chain to characterize system performance at the MAC layer. The authors also introduced a new metric, namely BSR (Buffer Status Rate) delivery rate, and described the tradeoff between offered network throughput and the capability to support new users. Analysis were validated through simulations.

Some researchers [7] have detailed a number of challenges facing 802.11ax implementation (e.g., OFDMA scheduler, dynamic adjustment of sensitivity threshold, and energy savings as an optimization problem between energy consumption and throughput).

In [10], Bellalta provided a review of expected applications and scenarios that call for a new amendment to existing standards, such as 802.11n and 802.11ac. A number of studies have also evaluated those two protocols from a systems level, providing insights on their physical-layer and MAC-layer efficiency [11], [12].

A Markov chain model was developed in [13] for estimating energy efficiency when increasing the contention window size for an 802.11ax node. Researchers also compared energy efficiency relative to the number of spatial streams for transmitting frames. This study reported that leveraging MU-MIMO (multi-user multiple-input multiple-output) optimized efficiency with four bandwidths offered by 802.11ax. Finally, researchers in [14] examined using 802.11ax for IoT, assuming that it is able to resolve energy efficiency and range problems.

The work presented in this paper focuses on application layer performance (e.g., throughput, delay, and packet loss) of 802.11ax under various conditions and provides empirical models of network performance for future deployments. The balance of this paper is organized as follows. Section II provides an overview of key features and enhancements of 802.11ax. Section III describes the experimental setup and software used for testing. Results and discussion are presented in Section IV, and the paper concludes in Section V.

II. IEEE 802.11AX AT A GLANCE

The new 802.11ax specification introduces significant changes to the physical and MAC layers of the protocol. A key change is the introduction of an Orthogonal Frequency-Division Multiple Access (OFDMA) approach, which is built on top of legacy CSMA/CA (Carrier Sense Multiple Access with Collision Avoidance). The standard was designed with a careful consideration for legacy specifications, 802.11a/b/g/n/ac that although challenging, it allows backward compatibility with earlier versions.

A. Physical Layer

The 802.11ax amendment allows access to the 2.4 GHz and 5.0 GHz bands; it also supports channel bandwidths up to 40 MHz at 2.4 GHz and up to 160 MHz at 5.0 GHz. By virtue of OFDMA, the channel subcarriers are grouped into units in time and frequency domains (i.e., resource units [RU]). This approach facilitates simultaneous communication with multiple receivers by mapping various RUs to different stations and avoids frequency selectivity by allocating a given station bandwidth as low as 2.5 MHz or 26 subcarriers. When compared with 64 subcarriers supported by the earlier 802.11ac standard, 802.11ax increases the number of subcarriers to 256, from which a maximum of 242 can be used. The remainder are reserved to decrease inter-symbol interference (ISI) and leakage from adjacent tones. The increased number of tones is accompanied by increased OFDM symbol duration to 12.8 μ s and selectable Guard Interval (GI) of 0.8, 1.6, or 3.2 μ s, which account for more robust outdoor operation.

The new amendment also introduces a higher modulation rate of 1024-QAM, in addition to those supported by 802.11ac; BPSK, 16-QAM, 64-QAM, and 256-QAM [15]. Moreover, the updated standard adds support for higher forward error correction rates of 1/2, 2/3, 3/4, and 5/6. The new physical layer offers an increased data rate of 25%

from 802.11ac, achieving 9.6 Gbps at a high Modulation and Coding Scheme (MCS) transmitted over 160 MHz or 80+80 MHz channel with eight spatial streams and 0.8 μ s GI.

B. Trigger Frame and Multi-User Transmission

802.11ax operates in either single- or multi-user fashion. The earlier 802.11ac standard previously supported downlink multi-user transmission (DL MU), leveraging multiple-input multiple-output (MIMO) technology. 802.11ax supplements functionality by multiplexing users in the uplink, as well. Uplink multi-user transmission (UL MU) is realized via the inherited multi-user MIMO (MU-MIMO) in 802.11ac and borrowing from the technological advancement of cellular technology in OFDMA. In both methods, the access point (AP) controls and orchestrates transmissions among stations within the network. Notably, MU-MIMO and OFDMA can be combined in an 802.11ax network.

The main challenge of the new standard is embodied in the UL MU transmission, namely synchronization among different stations when sending data simultaneously to the AP, as their clocks might drift as a result of jitter. Fortunately, the specification defines a new type of control frame, namely Trigger Frames, that AP sends to all users. This trigger frame initiates uplink transmission for all users for sending data or a response to multi-user block acknowledgment request (MU-BAR). Trigger frames include information about upcoming uplink transmission, such as duration, GI (identical for all participating UL MU transmission [16]) OFDMA resource allocation of RUs, per-station parameters (e.g., MCS, TX power, and others), and number of spatial streams.

C. OFDMA Random Access

Since AP controls and allocates RUs for stations transmitting in UL MU mode, there are occasions in which AP might be unaware of an associated station with data to send or an unassociated station desiring to join the Basic Service Set (BSS). Such short packet UL frames must be accounted for in a UL MU transmission. Because Distributed Coordination Function (DCF) scheme is otherwise inefficient and costly in terms of overhead, the 802.11ax specification was designed to address this issue by leveraging the OFDMA Back-off (OBO) procedure [17]. AP sends a special Trigger Frame, including information about random access RUs for stations without allocated resource elements, in which to transmit and contend for once awarded. A given station selects a random number in the range $[0, CWO]$ where CWO is the OFDMA contention window. Given that a station's OBO value is less than or equal to the number of random-access RUs declared in a Trigger Frame, one RU is randomly selected to transmit its frame. Otherwise, the OBO value is decreased by the number of declared RUs in the Trigger Frame and awaits the subsequent one. Given that the transmission fails, the station doubles its CWO and initializes its OBO value with a new random number from within the new range until CWO reaches CWO_{max} . Following successful transmission, the station resets its CWO to CWO_{min} .

D. BSS Coloring

Dense deployments are at the core of 802.11ax target scenarios. Sites with highly dense APs can experience co-channel interference from neighboring BSS. 802.11ax allows stations to determine whether a detected frame is originating from within its network or from its neighboring networks. By examining the BSS color bit in the frame header, a station can identify overlapping BSS (OBSS) and make decisions on medium interference management. According to the amendment, stations are allowed to adjust parameters related to Clear Channel Assessment (CCA) procedure to differentiate between intra- and inter-BSS frames without having to decode the entire frame. Moreover, the standard defines two Network Allocation Vectors (NAV) – one for the intra-BSS and another for inter-BSS stations. Hence, NAVs from OBSS cannot affect NAVs from within a station’s BSS. Therefore, 802.11ax exhibits improved spatial reuse behavior and spectrum resource management.

III. EMPIRICAL SETUP

An ASUS 802.11ax-enabled 4x4 MIMO router (i.e. access point [AP]) [18] was used in conjunction with a laptop equipped with an Intel AX200 2x2 MIMO wireless card [19] supporting 802.11ax implementation. AP was connected to another laptop over ethernet for generating traffic. The setup layout is depicted in Fig. 1.

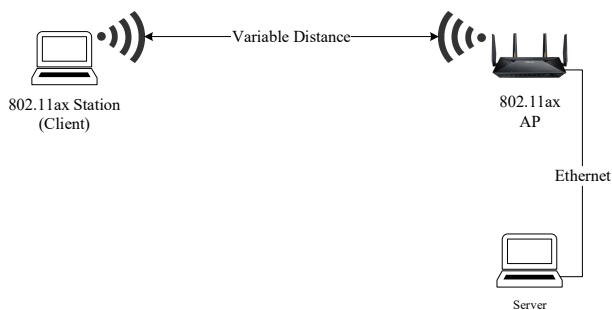


Fig. 1. Experimentation setup.

Tests were carried out in an office setting to resemble a real-world scenario. The station and AP were not connected to the Internet in an effort to prevent background traffic and limit interference that could affect measurements.

Signal-to-Noise Ratio (SNR) was varied by changing the separating distance between the station and the AP, since transmission power control was not accessible in the AP. Furthermore, to avoid interference from surrounding devices, all tests were conducted in the evenings or on weekends. Hence, it can be assumed the background noise was both minimal and constant throughout testing.

Various software tools were utilized for testing and data collection (e.g., delay, jitter, throughput, and packet loss rate, among others). iPerf3 [20] is a tool for investigating IP networks and taking active measurements on maximum achievable bandwidth. iPerf3 supports protocols, such as TCP, UDP, and SCTP, with IPv4 and IPv6; it also aids in tuning

network timing parameters. Wireshark [21] monitored traffic status. Netspot [22] and Acrylic WiFi [23] were utilized to assess the wireless connection and to collect measurements on RSSI and noise. MTR [24] is a network diagnosis tool that combines the functionalities of ‘traceroute’ and ‘ping’ and provides statistics on each route hop between host and destination address, in addition to information about channel state, connection state, and intermediate host responsiveness.

IV. 802.11AX PERFORMANCE ANALYSIS

Results of conducted tests are presented and discussed in this section. Measurements were repeated 10 times to ensure repeatability and minimum mean square error (MMSE). It is important to note that results could vary given alternative hardware implementation for the testing setup. That said, the results reported herein should be regarded as representative of available commercial devices implementing 802.11ax standard.

A. Throughput vs. SNR

Throughput is expected to increase as bandwidth and SNR increase. This was confirmed and is demonstrated in Fig. 2 and Fig. 3, which show TCP protocol throughput in downlink (Fig. 2) and uplink (Fig. 3).

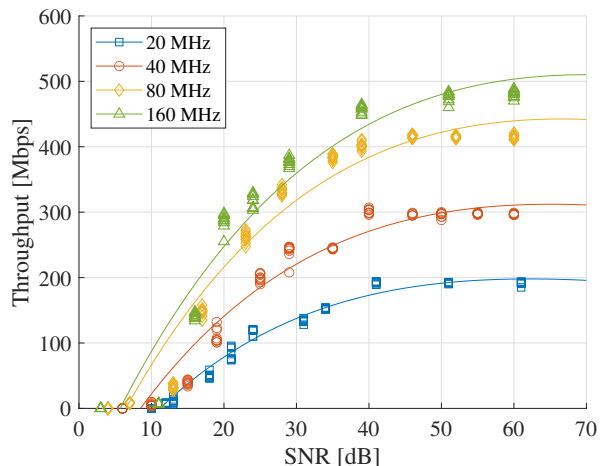


Fig. 2. Downlink throughput of 802.11ax node via TCP protocol.

Although downlink and uplink throughputs reach almost the same saturation limits using similar channel bandwidths, the uplink traffic under 160 MHz channel bandwidth acts differently. At 160 MHz, uplink traffic does not benefit from doubling the channel bandwidth, and saturation throughput is nearly the same for 80 MHz bandwidth, and sometimes lower. This can be attributed to differences in 802.11ax implementation, since client and server utilize different hardware. The relationship between throughput and SNR for downlink and uplink traffic can be characterized using an exponential model:

$$\theta = \alpha e^{\beta x} + \gamma e^{\delta x} \quad (1)$$

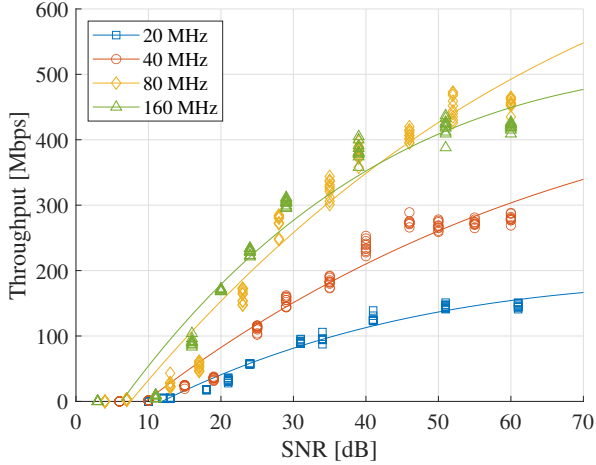


Fig. 3. Uplink throughput of 802.11ax node via TCP protocol.

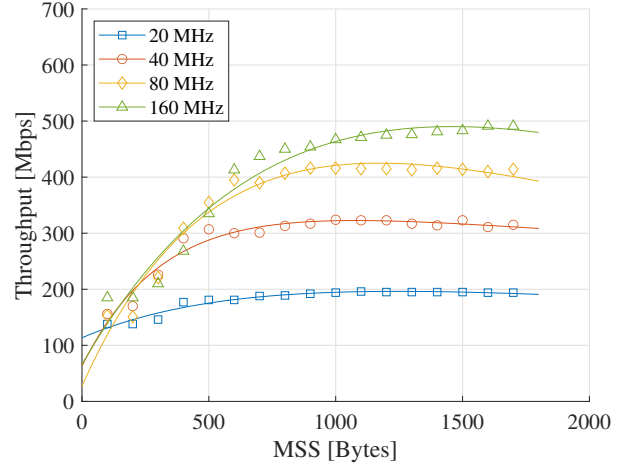


Fig. 4. TCP packet size effect on throughput.

TABLE I
TCP DOWNLINK AND UPLINK MODELS COEFFICIENTS.

		α	β	γ	δ	R^2
DL	20 MHz	1.365e+07	-0.01963	-1.365e+07	-0.01963	0.9815
	40 MHz	5.81e+06	-0.01767	-5.81e+06	-0.01767	0.9564
	80 MHz	-1.383e+07	-0.01662	1.383e+07	-0.01662	0.9545
	160 MHz	-2.459e+07	-0.01557	2.459e+07	-0.01557	0.9314
UL	20 MHz	-9.112e+06	-0.01123	9.112e+06	-0.01123	0.9750
	40 MHz	9.237e+06	-0.006891	-9.237e+06	-0.006892	0.9589
	80 MHz	-2.654e+08	-0.00672	2.654e+08	-0.00672	0.9569
	160 MHz	-2.005e+07	-0.01111	2.005e+07	-0.01111	0.9462

where θ is the downlink or uplink throughput; x is SNR; and α , β , γ , and δ are coefficients listed in Table I. Goodness-of-fit (R^2) is higher than 0.92 for those models, which indicates high correlation between measurement points.

B. Throughput vs. Packet Size

Data is transmitted via packet chunks, the largest being Maximum Transmission Unit (MTU). For most network interfaces and systems, MTU has a default value of 1500 bytes. Data packets larger than the defined MTU must be fragmented into smaller units before transmission. TCP and IPv4 protocols encapsulate user data in their protocol-specific headers when packets reach their respective network layer. Therefore, a TCP packet can carry up to 1460 bytes of user data. This is defined as TCP MSS (Maximum Segment Size), which is equal to MTU minus 40 bytes and accounts for TCP and IPv4 frame headers. In the testing scenario detailed in this paper, MSS was varied on the server side, and the client was running Wireshark to validate received payload length. SNR was ensured to be at least 60 dB during testing to eliminate noise effect on measured throughput. Fig. 4 shows the relationship between packet segment size and throughput.

As MSS increased, throughput increased until saturation throughput was achieved. It is interesting that given a 160 MHz channel, saturation throughput was reached when packet size was at least 1200 bytes. However, for all other channel bandwidths, critical MSS was approximately 800 bytes. This relationship can be quantified using the following exponential model:

$$\theta = \alpha e^{\beta m} + \gamma e^{\delta m} \quad (2)$$

where θ is the throughput; m is the segment size; α , β , γ , and δ are coefficients listed in Table II.

C. Throughput vs. Window Size

When a TCP connection is established between two nodes, namely a client and a server, both allocate a buffer to store data for reception and transmission. Operating systems control buffer size (i.e. windows) in a dynamic fashion to optimize network performance. A small window might underutilize the connection bandwidth, while a large window can block a huge amount of host memory, which, in turn, could degrade running application performance. Systems define default, minimum-, and maximum-allowed window sizes and employ algorithms, such as CUBIC [25], to dynamically control the window according to network congestion. iPerf3 allows modifying TCP connection window size. In the test scenario detailed herein, transmitter window/buffer size was increased from 10 bytes to 2 MB. Achieved throughput was measured while receiver window size remained fixed. Measurements were repeated for a fixed transmitter and a variable receiver window size. Fig. 5 and Fig. 6 illustrate results for various channel bandwidths. SNR was set high to ensure noise did not play a role in reported measurements.

Fig. 5 and Fig. 6 demonstrate the effect on throughput when changing transmitter and receiver window size, respectively. Both cases indicate that throughput under four channel bandwidths remains under 50 Mbps until buffer size reaches 10 KB. Subsequently, throughput increased proportionally

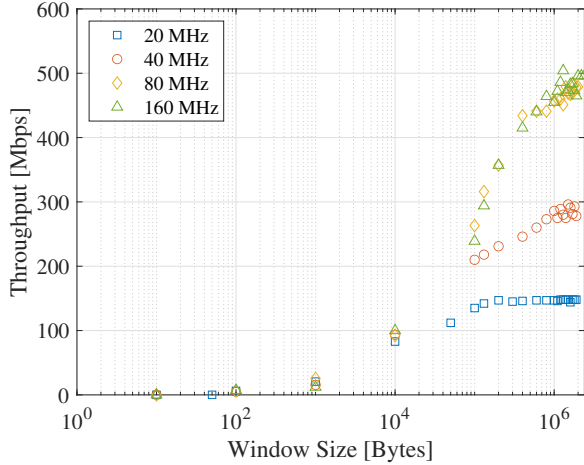


Fig. 5. Throughput performance as a function of transmitter's TCP window size.

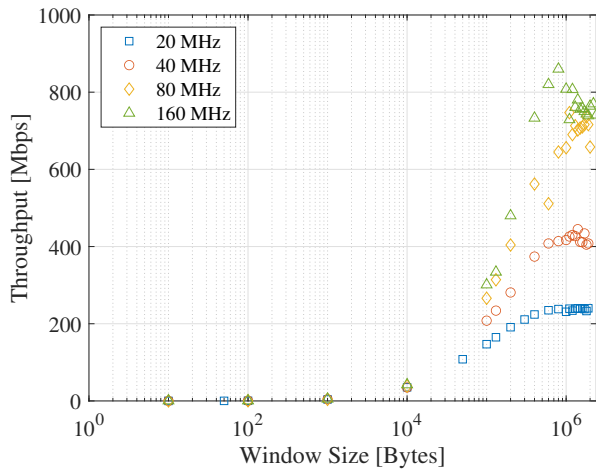


Fig. 6. Throughput performance as a function of receiver's TCP window size.

with window size until reaching saturation of approximately 1 MB. It is worth noting that given a 1 MB receiver window, maximum downlink throughput was 880 Mbps under a Linux operating system, while the same setting under a Windows operating system was 500 Mbps. This finding could be attributed to different TCP congestion control mechanisms and parameters implemented in the two operating systems.

D. Channel Occupancy

Duty cycle (DC) is a temporal measurement which is defined as the ratio of time the system signal exceeds an activity threshold over the entire observation time. In this test the channel utilization efficiency of 802.11ax wireless network is investigated. Fig. 7 plots the duty cycle of 802.11ax pair against achieved throughput in TCP downlink transmission for four channel bandwidths. As the channel bandwidth increased, the saturated throughput (indicated by maximum channel occupancy) increased as discussed earlier in Section IV-A. At a given throughput measurement, the utilization

decreased across the increasing channel bandwidths. This is an expected behavior since the bandwidth is doubled. Moreover, Fig. 7 demonstrates that 802.11ax exhibits better channel utilization than 802.11ac. DC of 802.11ax was nearly the same for 160 MHz and 80 MHz channel bandwidths up until 450 Mbps achieved throughput. After which, the utilization of 160 MHz channel improves over that of 80 MHz channel until saturation is achieved at 600 Mbps.

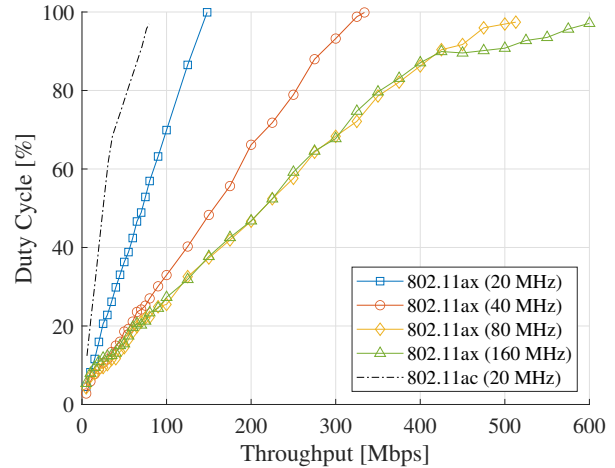


Fig. 7. Duty cycle of 802.11ax (four channels) and 802.11ac.

E. Jitter vs. SNR

Jitter can be conceptualized as the difference in received packet delays. At the sending side, packets are transmitted in a continuous stream with evenly distributed delays (i.e., time gaps) between packets. Network congestion (or queuing delay) in network hops causes the time difference between packets to vary. If jitter is too high in time-sensitive applications, such as voice or video stream, the jitter buffer is made large to compensate. Fig. 8 shows the relationship between receiver SNR and jitter measured using UDP link. The figure also indicates standard deviation for each measurement.

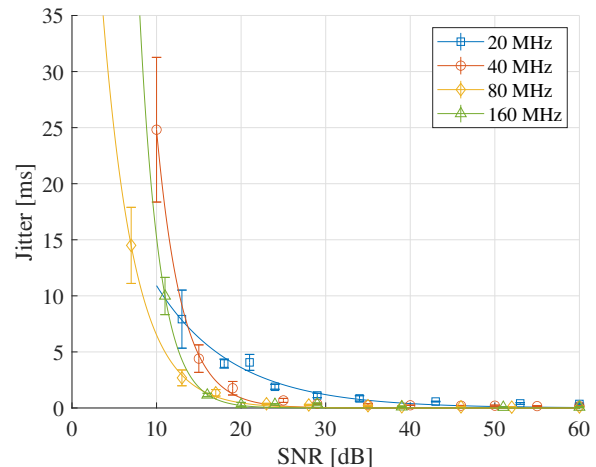


Fig. 8. 802.11ax jitter with various SNR using UDP link.

TABLE III
COEFFICIENTS AND GOODNESS OF FIT OF JITTER VS. SNR MODEL.

	α	β	R^2
20 MHz	33.03	-0.1108	0.9705
40 MHz	685	-0.3319	0.9982
80 MHz	93.36	-0.2663	0.9982
160 MHz	1028	-0.4213	0.9973

Overall, jitter in four bandwidths decreased as SNR increased. Two phenomena can be observed from the jitter-SNR relationship. First, jitter remains lower than 5 ms when SNR increases from 20 dB to 60 dB, although jitter is typically shorter than 1 ms. Second, the jitter curve can be characterized by an exponential behavior, described in (3) and Table III.

Based on the setup for this investigation, the router served only two laptops. Therefore, one can surmise that jitter is mainly due to packets lost as a result of low SNR.

$$\tau = \alpha e^{\beta x} \quad (3)$$

τ is jitter; x is SNR; and α and β are constant coefficients.

V. CONCLUSION

Prospective technologies pose challenging requirements on next-generation wireless communication systems and must be quickly addressed to ensure a successful roll out. Several global standardization governing bodies and consortiums are tirelessly releasing novel features and enhancements to current protocols or proposing innovative protocols in an attempt to swiftly adapt to future demands. 802.11ax or Wi-Fi 6 is one such solution proposed by the IEEE and Wi-Fi Alliance for meeting needs in the unlicensed band.

This work highlights an empirical investigation of new amendment performance from an application layer perspective. A multitude of tests were conducted to investigate a number of metrics (e.g., throughput and jitter) and their relationship with parameters (e.g., payload length and environment variables, such as SNR). Empirical models were developed using test results to quantify the behavior of said metrics. Fitting accuracy was 0.95 on average. Channel occupancy of the system was investigated as well. Results show that not only 802.11ax achieves higher throughput than its precedent, 802.11ac, but also exhibits a better channel utilization by virtue of its higher MCS.

REFERENCES

- [1] Aruba, "The Wi-Fi Market and the genesis of 802.11ax," 2018. [Online]. Available: https://www.arubanetworks.com/assets/wp/WP_802.11AX.pdf
- [2] Ericsson, "Future mobile data usage and traffic growth," 2019. [Online]. Available: <https://www.ericsson.com/en/mobility-report/future-mobile-data-usage-and-traffic-growth>
- [3] A. Mourad, S. Muhammad, M. O. Al Kalaa, P. A. Hoehner, and H. Refai, "Bluetooth and IEEE 802.11n system coexistence in the automotive domain," in *IEEE Wireless Communications and Networking Conference, WCNC, 2017*.
- [4] A. Mourad, S. Muhammad, M. O. Al Kalaa, H. H. Refai, and P. A. Hoehner, "On the performance of WLAN and Bluetooth for in-car infotainment systems," *Vehicular Communications*, vol. 10, no. August, pp. 1–12, oct 2017.

- [5] A. Algedir and H. H. Refai, "Adaptive d2d resources allocation underlying (2-tier) heterogeneous cellular networks," in *2017 IEEE 28th Annual International Symposium on Personal, Indoor, and Mobile Radio Communications (PIMRC)*, Oct 2017, pp. 1–6.
- [6] F. Aveta, H. H. Refai, and P. LoPresti, "Multi-user FSO communication link," in *2017 Cognitive Communications for Aerospace Applications Workshop, CCAA 2017*. IEEE Inc., aug 2017.
- [7] E. Khorov, A. Kiryanov, A. Lyakhov, and G. Bianchi, "A Tutorial on IEEE 802.11ax High Efficiency WLANs," *IEEE Communications Surveys & Tutorials*, vol. 21, no. 1, pp. 197–216, 2019.
- [8] Q. Qu, B. Li, M. Yang, and Z. Yan, "An OFDMA based concurrent multiuser MAC for upcoming IEEE 802.11ax," in *2015 IEEE Wireless Communications and Networking Conference Workshops (WCNCW)*. IEEE, mar 2015, pp. 136–141.
- [9] G. Naik, S. Bhattarai, and J.-M. Park, "Performance Analysis of Uplink Multi-User OFDMA in IEEE 802.11ax," in *2018 IEEE International Conference on Communications (ICC)*, vol. 2018-May. IEEE, may 2018, pp. 1–6.
- [10] B. Bellalta, "IEEE 802.11ax: High-efficiency WLANs," *IEEE Wireless Communications*, vol. 23, no. 1, pp. 38–46, feb 2016.
- [11] S. A. Rajab, W. Balid, and H. H. Refai, "Comprehensive study of spectrum occupancy for 802.11b/g/n homogeneous networks," in *Conference Record - IEEE Instrumentation and Measurement Technology Conference*, vol. 2015-July. IEEE Inc., jul 2015, pp. 1741–1746.
- [12] N. Mostahinic and H. Refai, "Spectrum occupancy for 802.11a/n/ac homogeneous and heterogeneous networks," in *2019 15th International Wireless Communications and Mobile Computing Conference, IWCMC 2019*. IEEE Inc., jun 2019, pp. 1690–1695.
- [13] Z. Machrouh and A. Najid, "High efficiency IEEE 802.11ax MU-MIMO and frame aggregation analysis," in *2018 International Conference on Advanced Communication Technologies and Networking (CommNet)*. IEEE, apr 2018, pp. 1–5.
- [14] M. S. Afaqui, E. Garcia-Villegas, and E. Lopez-Aguilera, "IEEE 802.11ax: Challenges and Requirements for Future High Efficiency WiFi," *IEEE Wireless Communications*, vol. 24, no. 3, pp. 130–137, jun 2017.
- [15] E. Park, J. Choi, J. Chun, D. Lim, J. Kim, S. Kim, H. Choi, and H. Cho, "1024 QAM Proposal," 2015. [Online]. Available: <https://mentor.ieee.org/802.11/dcn/15/11-15-1070-03-00ax-1024-qam-proposal.ppt>
- [16] Z. Rong, Y. Yang, P. Loc, L. Liu, J. Luo, Y. Luo, and Y. Lin, "CP Indication for UL MU Transmission," 2015. [Online]. Available: <https://mentor.ieee.org/802.11/dcn/15/11-15-0813-00-00ax-cp-indication-for-ul-mu-transmission.pptx>
- [17] C. Ghosh, R. Stacey, E. Perahia, S. Azizi, P.-K. Huang, Q. Li, L. Cariou, and X. Chen, "UL OFDMA-based Random Access Procedure," 2015. [Online]. Available: <https://mentor.ieee.org/802.11/dcn/15/11-15-1105-00-00ax-ul-ofdma-based-random-access-procedure.pptx>
- [18] Asus, "ASUS RT-AX88U Router." [Online]. Available: <https://www.asus.com/us/Networking/RT-AX88U/>
- [19] Intel, "Intel Wi-Fi 6 AX200." [Online]. Available: <https://ark.intel.com/content/www/us/en/ark/products/189347/intel-wi-fi-6-ax200.html>
- [20] "iPerf." [Online]. Available: <https://iperf.fr/>
- [21] "Wireshark." [Online]. Available: <https://www.wireshark.org/>
- [22] "Netspot." [Online]. Available: <https://www.netspotapp.com/>
- [23] "Acrylic WiFi." [Online]. Available: <https://www.acrylicwifi.com/en/>
- [24] "MTR." [Online]. Available: <http://www.bitwizard.nl/mtr/>
- [25] S. Ha, I. Rhee, and L. Xu, "CUBIC: A new TCP-friendly high-speed TCP variant," in *Operating Systems Review (ACM)*, vol. 42, no. 5, jul 2008, pp. 64–74.